Proceeding of the 6th International Symposium on Artificial Intelligence and Robotics & Automation in Space: i-SAIRAS 2001, Canadian Space Agency, St-Hubert, Quebec, Canada, June 18-22, 2001.

Planning and Control Algorithms for Enhanced Rough-Terrain Rover Mobility

Karl Iagnemma*, Hassan Shibly+, Adam Rzepniewski*, Steven Dubowsky*

*Massachusetts Institute of Technology
Department of Mechanical Engineering
Cambridge, MA 02139 USA kdi@mit.edu

+Mechanical Engineering Department
Bir-Zeit University
Palestinian Territories

Keywords: Rovers, Planetary Exploration, Surface Systems, Rough-Terrain, Motion Planning, Robot Control

Abstract

Future planetary exploration missions will require rovers to perform difficult tasks in rough terrain, with limited human supervision. Many current motion planning and control algorithms do not consider the physical characteristics of the rover and its environment, which limits their effectiveness in rough terrain. This paper presents an overview of physics-based rover and terrain modeling techniques that allow improved prediction of rough-terrain rover mobility. Kinematic and force models of a rover in rough terrain are presented. A method for on-line estimation of critical terrain physical parameters is presented. A method for on-line estimation of wheel-terrain contact geometry is also presented. It is shown that these modeling techniques can be used in advanced control and motion planning algorithms to improve a rover's rough-terrain mobility.

1. Introduction

In NASA's recent Pathfinder mission, the Sojourner rover was limited to short traverses in relatively benign terrain under constant human supervision. Future planetary exploration missions will require rovers to perform difficult mobility tasks in rough terrain, with limited human supervision [6, 14]. Current rover motion planning and control algorithms are not well suited to rough-terrain, since they generally do not consider the physical capabilities of the rover in its environment. Without capability for on-line prediction of a rover's performance, the system must act conservatively to avoid danger. This limits the ability of a rover to attempt acquisition of valuable science targets that may lie on steep hillsides, in ravines, etc.

To meet future mission requirements, advanced control and planning methods must be developed that consider the physical characteristics of the rover and its environment, and thus fully utilize the rover's physical capabilities. This paper presents an overview of physics-based modeling techniques for planetary exploration rovers operating in rough terrain. These models can then be used as a basis for advanced control and motion planning methods to improve a rover's rough-terrain mobility.

The "physics-based" research approach described in this paper is illustrated in Figure 1. This approach is in contrast to the "black box" approach of many control and motion planning methods, which use limited or no physical system information. In the physics-based approach, both the rover and its environment are carefully modeled to ensure accurate prediction of the system's capabilities.

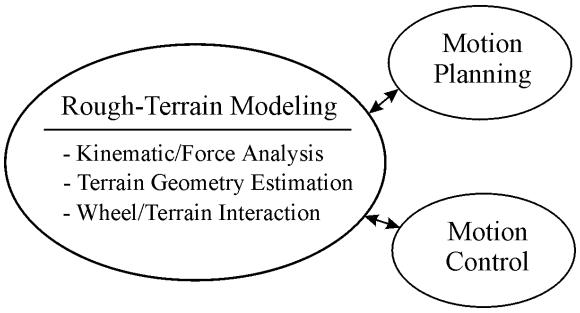

Figure 1: Physics-based approach

The modeling techniques presented in this paper are divided into two sections: rover models and terrain models. In Section 2, methods for formulating rover models are presented. First, a method for formulating a classical kinematic model of a rover in rough terrain is presented. A method for formulating a quasi-static model of forces acting on the rover wheels, suspension, and manipulator is also presented. Note that quasi-static models are appropriate for current planetary exploration rovers, due to their slow speeds. These models are computationally simple, and thus practical for on-board implementation.

In Section 3, methods for formulating terrain models are presented. First, a method for on-line estimation of critical terrain parameters is presented [12]. Wheel-terrain interaction has been shown to play a significant role in rough-terrain mobility [2]. On-line estimation of terrain parameters is important, since this allows a rover to adapt its planning and control strategies to a given terrain. For example, a rover traveling over loose soil should behave differently than a rover traveling over firm clay. In this paper a method is presented that uses on-board sensors and is computationally simple.

Second, a method for on-line estimation of wheel-terrain contact geometry is presented [9]. Wheel-terrain contact angles are important elements of a rover model, as these angles greatly influence rover force application properties. For example, a rover traversing flat, even terrain has different mobility characteristics than one traversing steep, uneven terrain. The method presented here uses simple, on-board sensors and an extended Kalman filter to fuse noisy signals.

The modeling techniques presented in this paper form a basis for motion planning and control algorithms that fully exploit a rover's capabilities. These algorithms include a rough-terrain control algorithm and a planning algorithm that adjusts the configuration of an articulated suspension rover to maximize tip-over stability. Results from these algorithms are briefly presented in Section 4 [8, 9, 10, 11].

2. Rover Modeling

Here, two rover modeling techniques are presented and briefly discussed. The first is a classical kinematic model. The second is a quasi-static model of forces acting on the rover wheels, suspension, and manipulator.

1.1 Rover Kinematic Model

Kinematic analysis is an important aspect of rover mobility prediction. However, solving the inverse kinematic problem of a multi-wheeled rover systems in rough terrain is nontrivial. Here, an analysis of an example system (a six-wheeled rocker-bogie rover) is summarized [2] (see Figure 2). This example problem illustrates many of the inherent difficulties in modeling multi-wheeled rover systems in rough terrain.

To fully define the rover configuration, ten parameters are required: the position of the center of mass of the body $\mathbf{p}_c = [p_x\ p_y\ p_z]^T$, the orientation of the rover body (Θ, Φ, Ψ), and the configuration parameters of the rocker-bogie mechanism $(\theta_{1r}, \theta_{2r}, \theta_{1l}, \theta_{2l})$. The inverse kinematics problem for this rover involves computing the orientation (Θ, Φ, Ψ) of the rover body and the configuration $(\theta_{1r}, \theta_{2r}, \theta_{1l}, \theta_{2l})$ of the rover suspension, given the shape of the terrain and the position of the center of the body $\mathbf{p}_c$.

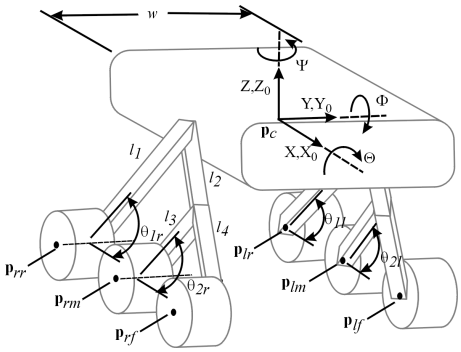

Figure 2: Kinematic description of a six-wheeled rover

For a vehicle with m unique wheel-terrain contact points, at least m-1 kinematic loop closure equations can be written [4]. For the rover shown in Figure 2, these loop closure equations are:

$$z_{rr} = z_{lr} + l_1 \cos\Theta(\sin\theta_{1r} - \sin\theta_{1l}) + w\sin\Theta \quad (1)$$

$$z_{rr} = z_{lm} + \cos\Theta(l_1 \sin\theta_{1r} - l_2 \cos\theta_{1l} - l_3 \sin\theta_{2l}) + w\sin\Theta \quad (2)$$

$$z_{rr} = z_{lf} + \cos\Theta(l_1 \sin\theta_{1r} - l_2 \cos\theta_{1l} - l_4 \cos\theta_{2l}) + w\sin\Theta \quad (3)$$

$$z_{rr} = z_{rm} + \cos\Theta(l_1 \sin\theta_{1r} - l_2 \cos\theta_{1r} - l_3 \sin\theta_{2r}) \quad (4)$$

$$z_{rr} = z_{rf} + \cos\Theta(l_1 \sin\theta_{1r} - l_2 \cos\theta_{1r} - l_4 \cos\theta_{2r}) \quad (5)$$

where z_{ij}, $i = \{r,l\}$, $j = \{r,m,f\}$ refers to the z component of $\mathbf{p}_{ij}$, with index i referring to the right or left side, and index j referring to the rear, middle, or front wheel. Due to the mechanical differential in this system, an additional equation can be written relating the pitch Φ to the angles θ_{1r} and θ_{1l}:

$$\Phi = (\theta_{1r} + \theta_{1l})/2 + \theta'_{1r} \quad (6)$$

where θ'_{1r} is the value of θ_{1r} when the rover is on flat terrain. Thus, six unique kinematic equations can be written for the rover in Figure 2.

Inputs to the problem are assumed to be a terrain elevation map, the position $\mathbf{p}_c$ of the rover center, and the rover heading Ψ. Position and heading are taken as inputs since the goal of kinematic analysis is often to predict the traversability and stability at a given point in the terrain map. These inputs reduce the number of unknown parameters to six, which can be determined by solving the nonlinear system of Equations (1-6).

Numerical techniques such as Newton's method and steepest descent can be applied to this problem, although convergence is not guaranteed since the terrain elevation map is generally not represented by a continuously differentiable function. A solution method for rover inverse kinematics have been presented that rely on simplifying assumptions about the rover configuration [3, 5]. An analytical technique for solving position kinematics of multi-module robot systems has been presented [16]. In general, computation of the inverse kinematic solution of a multi-wheeled vehicle on uneven terrain is nontrivial.

1.2 Rover Force Analysis

Force analysis is another important aspect of rover mobility prediction. In this section a force analysis of a six-wheeled rover with a rocker-bogie suspension is presented. Here it is assumed that no moments exist at the wheel-terrain contact points, a reasonable assumption for natural terrain [2].

Figure 3 is a diagram of a six-wheeled mobile robot on uneven terrain. The vectors $\mathbf{f}_i$ represent wheel-terrain interaction forces. The vectors $\mathbf{p}_i$ are directed from the wheel-terrain contact points to the rover center of mass. The vector $\mathbf{f}_s$ at the rover center of mass represents the summed effects of gravitational forces, inertial forces, forces due to manipulation, and forces due to interaction with the environment or other robots. Note that rover link, wheel and body masses are lumped at the center of mass. Note also that $\mathbf{f}_s$ can possesses a user-specified component in the direction of desired motion.

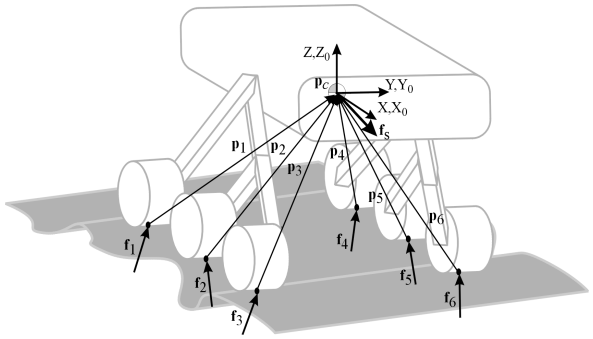

Figure 3: Force analysis of a six-wheeled rover

A set of quasi-static force balance equations for the six-wheeled rover shown in Figure 3 can be written as:

$$\begin{bmatrix} \mathbf{I} & \cdots & \mathbf{I} \\ 0 & p_1^z & p_1^y & \cdots & 0 & p_6^z & p_6^y \\ -p_1^z & 0 & -p_1^x & \cdots & -p_6^z & 0 & -p_6^x \\ -p_1^y & p_1^x & 0 & & -p_6^y & p_6^x & 0 \end{bmatrix} \begin{bmatrix} \mathbf{f}_1 \\ \vdots \\ \mathbf{f}_6 \end{bmatrix} = \mathbf{f}_s \qquad (7)$$

where $\mathbf{I}$ represents a 3 x 3 identity matrix. This set of equations can be written in compact matrix form as:

$$\mathbf{G}\mathbf{x} = \mathbf{f}_s \qquad (8)$$

Equation set (8) is generally referred to as the force distribution equations [7]. This set of equations represents 6 equations in 18 unknowns. Thus, the force analysis problem is underconstrained, and there exists an infinite set of wheel-terrain contact force vectors $\mathbf{f}_i$ that balance the body vector $\mathbf{f}_s$. In general, a force analysis of an m-wheeled rover will yield six equations in $3m$ unknowns, and thus the force analysis problem will be underconstrained except for the trivial case of a two-wheeled vehicle.

Solution methods of the force distribution equations have been discussed in [12, 15]. In general, a solution to the wheel-terrain contact force vector $\mathbf{x}$ is found that optimizes a user-defined criteria, such as power consumption, traction, etc.

Note that the amount of force that can be applied at the wheel-terrain contact force is limited by the actuator saturation level and the terrain strength [2]. Additionally, the force vector $\mathbf{x}$ must contain a component that is directed normal to the terrain, as this ensures that all wheels remain in contact with the terrain. These limitations can be viewed as constraints on the solution of Equation 8. The maximum terrain strength can be determined by Coulomb theory as $\tau = A(c + \sigma \tan\phi)$ where A is the projected wheel area, c is the terrain cohesion, σ is the normal stress at the wheel-terrain interface, and ϕ is the internal friction angle [2].

Failure to find a vector of wheel-terrain contact forces $\mathbf{x}$ that satisfy Equation 8 implies that the rover cannot move in the direction of desired motion. Conversely, a large space of solutions for $\mathbf{x}$ implies that the terrain is highly traversable. Thus, force analysis is an important part of rover traversability evaluation.

3. Terrain Modeling

Here, two terrain modeling techniques are presented and briefly discussed. The first is a method for terrain parameter estimation. The second is a method for terrain geometry estimation.

3.1 On-Line Terrain Parameter Estimation

Wheel-terrain interaction has been shown to play a significant role in rough-terrain mobility [2]. Thus, it is important to be able to estimate the values of critical terrain parameters, in order to accurately predict rover mobility. Here, the case of a smooth rigid wheel traveling through deformable terrain is considered, as this is the expected condition for planetary exploration vehicles. A more detailed treatment of this method is presented in [12].

To estimate terrain parameters, equations relating the parameters of interest to physically measurable quantities must be developed. The physical parameters of interest are the terrain cohesion c and the internal friction angle ϕ. Knowledge of these parameters allows estimation of the maximum stress a soil region can bear, which is important in traversability analysis [2].

A free-body diagram of a driven rigid wheel traveling through deformable terrain is shown in Figure 4. A vertical load W and drawbar pull DP are applied to the wheel by the vehicle suspension. A torque T is applied at the wheel rotation axis by an actuator. The wheel has angular velocity ω, and the wheel center possesses a linear velocity, V. The angle from the vertical at which the wheel first makes contact with the terrain is denoted θ_1. The angle from the vertical at which the wheel loses contact with the terrain is denoted θ_2.

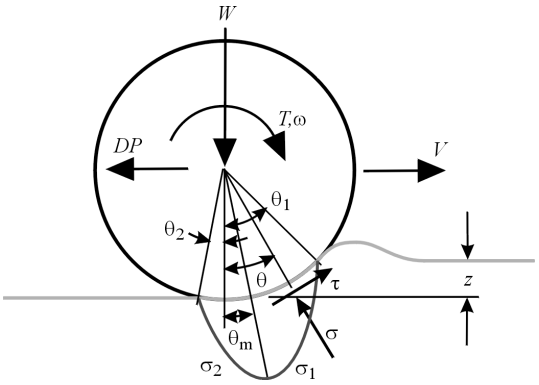

Figure 4: Rigid wheel on deformable terrain

The vertical load W and the torque T are assumed to be known quantities, since W can be computed from a static analysis of the rover and T can be estimated from the current input to the wheel motor. A stress region is created at the wheel-terrain interface, and is indicated by σ_1 and σ_2. The angle from the vertical at which the maximum stress occurs is denoted θ_m.

From Figure 4, force balance equations can be written as:

$$W = rb\left(\int_{\theta_2}^{\theta_1}\sigma(\theta)\cos\theta\cdot d\theta + \int_{\theta_2}^{\theta_1}\tau(\theta)\sin\theta\cdot d\theta\right) \quad (9)$$

$$DP = rb\left(\int_{\theta_2}^{\theta_1}\tau(\theta)\cos\theta\cdot d\theta - \int_{\theta_2}^{\theta_1}\sigma(\theta)\sin\theta\cdot d\theta\right) \quad (10)$$

$$T = r^2 b\int_{\theta_2}^{\theta_1}\tau(\theta)\cdot d\theta \quad (11)$$

Note that the shear stress τ and normal stress σ are functions of c and ϕ, among other variables [13]. Analytical solutions of Equations (9-11) are required to obtain closed-form expressions for c and ϕ. However, the complexity of these equations motivates the use of an approximate form of the fundamental stress equations.

Figure 5 is a plot of the shear and normal stress distributions around the rim of a driven rigid wheel on deformable terrain for varying sinkage coefficients n. The shear and normal stress distribution curves are approximately triangular for a wide range of n [17]. Based on this observation, a linear approximation of the shear and normal stress distribution equations can be written.

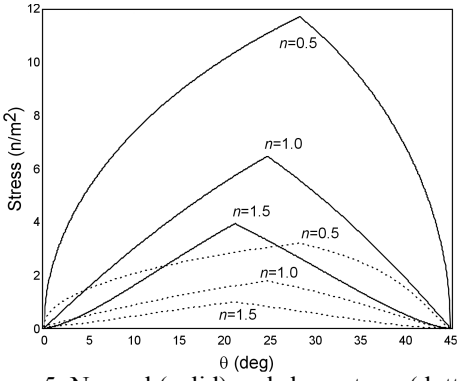

Figure 5: Normal (solid) and shear stress (dotted) distribution around driven rigid wheel

Simplified forms of the force balance equations can now be written and solved for the normal load W and torque T:

$$W = \left(rb/\theta_m(\theta_1-\theta_m)\right)\left[\begin{array}{l}\sigma_m(\theta_1\cos\theta_m-\theta_m\cos\theta_1-\theta_1+\theta_m)\\+\tau_m(\theta_1\sin\theta_m-\theta_m\sin\theta_1)\end{array}\right] \quad (12)$$

$$T = \frac{1}{2}r^2 b\tau_m\theta_1 \quad (13)$$

An additional equation can be written if the location of the maximum shear and normal stress are assumed to occur at the same location θ_m:

$$\tau_m = (c+\sigma_m\tan\phi)\left(1-e^{-\frac{r}{k}[\theta_1-\theta_m-(1-i)(\sin\theta_1-\sin\theta_m)]}\right) \quad (14)$$

where i is the wheel slip and is defined by i=1-$(V/r\omega)$.

The simplified equations can be solved for the cohesion and internal shear angle. Figures 6 and 7 show the results of estimation experiments that were performed with a six-wheeled laboratory rover.

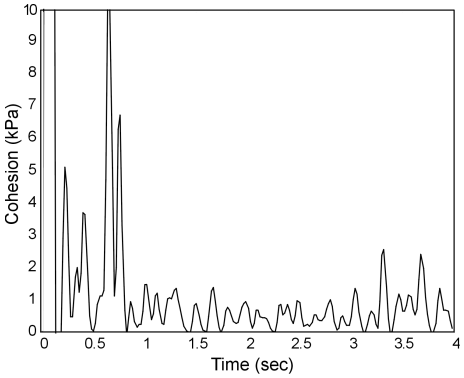

Figure 6: Estimated soil cohesion c by six-wheeled rover

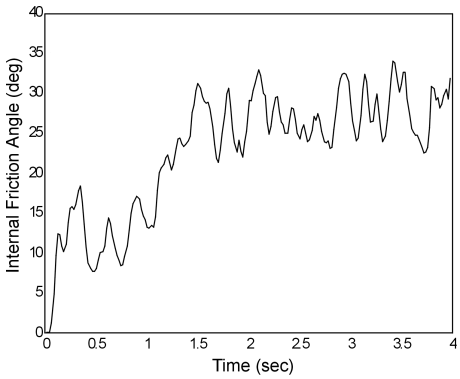

Figure 7: Estimated friction angle ϕ by six-wheeled rover

These results agree closely with those obtained with an instrumented wheel-terrain testbed (see Figure 8).

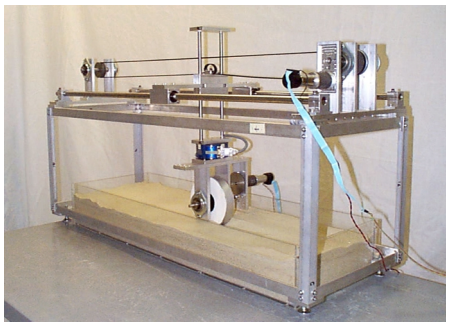
Figure 8: Wheel-terrain testbed

3.2 Wheel-Terrain Contact Angle Estimation

Wheel-terrain contact angles are important elements of a rover model, as these angles greatly influence rover force application properties. Here a method for wheel-terrain contact angle estimation is presented that uses simple, on-board sensors. A more detailed treatment of this method is presented in [9].

Consider a planar two-wheeled system on uneven terrain, see Figure 9. In this analysis the terrain is assumed to be rigid, and the wheels are assumed to make point contact with the terrain.

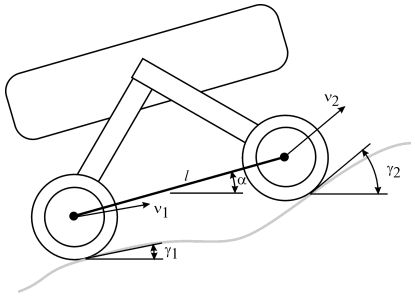

Figure 9: Planar system on uneven terrain

In Figure 9 the rear and front wheels make contact with the terrain at angles γ_1 and γ_2 from the horizontal, respectively. The vehicle pitch, α, is also defined with respect to the horizontal. The wheel centers have speeds v_1 and v_2. The distance between the wheel centers is defined as l.

For this system, the following kinematic equations can be written:

$$v_1 \cos(\gamma_1 - \alpha) = v_2 \cos(\gamma_2 - \alpha) \quad (15)$$

$$v_2 \sin(\gamma_2 - \alpha) - v_1 \sin(\gamma_1 - \alpha) = l\,\dot{\alpha} \quad (16)$$

Equation (15) represents the kinematic constraint that the wheel center length l does not change. Equation (16) is a rigid-body kinematic relation between the velocities of the wheel centers and the vehicle pitch rate $\dot{\alpha}$.

Combining Equations (15) and (16) yields:

$$\sin(\gamma_2 - \alpha - (\gamma_1 - \alpha)) = l\,\dot{\alpha}/v_1 \cos(\gamma_2 - \alpha) \quad (17)$$

With the definitions:

$$\theta \equiv \gamma_2 - \alpha, \quad \beta \equiv \alpha - \gamma_1, \quad a \equiv l\,\dot{\alpha}/v_1, \quad b \equiv v_2/v_1$$

Equations (15) and (17) become:

$$(b\sin\theta + \sin\beta)\cos\theta = a\cos\theta \quad (18)$$

$$\cos\beta = b\cos\theta \quad (19)$$

Solving Equations (18) and (19) for the wheel-terrain contact angles γ_1 and γ_2 yields:

$$\gamma_1 = \alpha - \cos^{-1}(h) \quad (20)$$

$$\gamma_2 = \cos^{-1}(h/b) + \alpha \quad (21)$$

where:

$$h \equiv (1/2a)\sqrt{2a^2 + 2b^2 + 2a^2b^2 - a^4 - b^4 - 1}$$

The pitch and pitch rate can be easily measured with rate gyroscopes or simple inclinometers. The wheel center speeds can be estimated from the wheel angular rate as measured by a tachometer, provided the wheels do not have substantial slip. Thus, wheel-terrain contact angles can be estimated with common, low-cost on-board sensors. However, sensor noise and wheel slip will degrade these measurements.

Here, an extended Kalman filter (EKF) is developed to compensate for these effects. This filter is an effective framework for fusing data from multiple noisy sensor measurements to estimate the state of a nonlinear system [18]. In this case the sensor signals are wheel tachometers, gyroscopes, and inclinometers, and are assumed to be corrupted by unbiased Gaussian white noise with known covariance. Inputs to the EKF are a system matrix **F**, a measurement matrix **H**, process and measurement error covariance matrices **Q** and **R**, and an initial state and covariance estimate. The EKF computes a minimum mean square estimate of the state vector **x**, which is composed of the wheel-terrain contact angles γ_1 and γ_2, the wheel center velocities v_1 and v_2, and the vehicle pitch α and pitch rate $\dot{\alpha}$, i.e. $\mathbf{x} = [\alpha \;\; \dot{\alpha} \;\; v_1 \;\; v_2 \;\; \gamma_1 \;\; \gamma_2]^T$. Note that speeds v_1 and v_2 can be approximated from knowledge of the wheel angular velocities and radii. The EKF system matrix **F** is a model of the nonlinear system, linearized about the

last state estimate. Here, the nonlinear equations describing the wheel-terrain contact angle estimation (Equations (7-8)) are linearized to form **F**. The system measurement matrix **H** relates the state **x** to the vector **z** of physically measured quantities v_1, v_2, α and $\dot{\alpha}$.

Computation of the EKF involves the following steps: 1) Initialization of the state **x** and an error covariance matrix **P**, 2) Propagation of the current state estimate and covariance matrix **P** at a given timestep *k*. The state estimate is computed as:

$$\mathbf{x}_{k+1} = \mathbf{F}_k \mathbf{x}_k \tag{22}$$

The covariance matrix **P** is computed as:

$$\mathbf{P}_{k+1} = \mathbf{F}_k \mathbf{P}_k \mathbf{F}_k^T + \mathbf{Q}_k \tag{23}$$

3) Updating state estimate and covariance matrix as:

$$\mathbf{x}_k^+ = \mathbf{x}_k + \mathbf{K}_k \left(\mathbf{z}_k - \mathbf{H}_k \mathbf{x}_k \right) \tag{24}$$

and

$$\mathbf{P}_k^+ = \left(\mathbf{I} - \mathbf{K}_k \mathbf{H}_k \right) \mathbf{P}_k \tag{25}$$

where the Kalman gain matrix **K** is given by:

$$\mathbf{K}_k = \mathbf{P}_k \mathbf{H}_k^T \left(\mathbf{H}_k \mathbf{P}_k \mathbf{H}_k^T + \mathbf{R}_k \right)^{-1} \tag{26}$$

See Figure 10 for a pictorial diagram of the EKF estimation process.

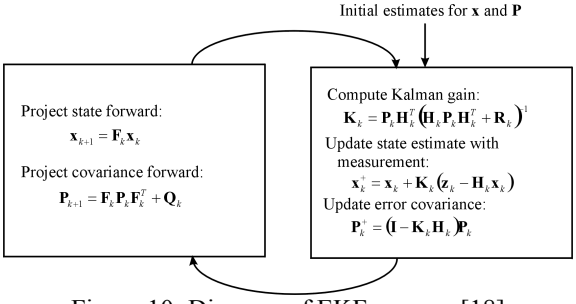

Figure 10: Diagram of EKF process [18]

Figure 11 shows results of wheel-terrain contact angle estimation experiments that were performed with a six-wheeled laboratory rover. In this experiment the front wheel of a rover begins traversing a 20º incline, while the middle and rear wheel remain on flat terrain. It can be seen that the algorithm does a good job estimating wheel-terrain contact angles using on-board sensors.

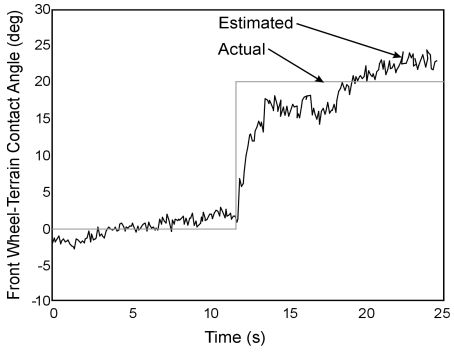

Front wheel

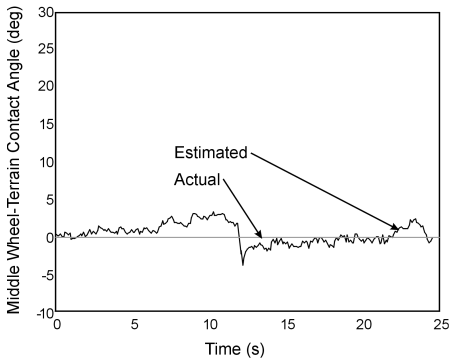

Middle wheel

Figure 11: Estimated terrain contact angles, 20º incline

4. Applications: Physics-Based Control and Planning Algorithms

The modeling and estimation techniques presented above form a basis of motion planning and control algorithms that fully exploit a rover's capabilities. These algorithms include a rough-terrain control algorithm, and a planning algorithm that adjusts the configuration of an articulated suspension rover to maximize tip-over stability. Results from these algorithms are briefly presented here. More details can be found in [8, 9, 10, 11, 12].

4.1 Rough-Terrain Control

A rough-terrain control method has been developed that utilizes simple sensory inputs to optimize for maximum wheel traction or minimum power consumption, depending on local terrain difficulty [10]. The algorithm exploits the fact that most rovers possess more wheel actuators than is minimally required to drive forward. This is seen mathematically in the underconstrained nature of the force distribution equations (Equation set 8). Thus, the traction control algorithm finds a set of wheel torques that satisfy the force distribution equations while maximizing wheel traction or minimizing power consumption.

To optimize for maximum traction, a function *R* that represents the maximum ratio of the tractive force to the normal force is minimized:

$$R = \max_i \left\{ T_i / N_i \right\} \tag{27}$$

where T_i represents the component of the i^{th} wheel's force vector that is tangent to the wheel at the wheel-terrain contact point, and N_i represents the component of the *i*th wheel's force vector that is normal to the wheel at the wheel-terrain contact point. Physically, minimizing *R* is equivalent to diminishing the force ratio of the wheel closest to soil failure.

To optimize for minimum power consumption, a function *P* that represents the relation between the wheel input torques and the power consumption is minimized:

$$P = \sum_{i=1}^{n} \left(R_i r_i^2 / K_i^{t\,2} N_i^2 \right) T_i^2 \qquad (28)$$

To determine which criteria to optimize for, a switching function based on the estimated wheel-terrain contact angles is developed, as:

$$S = \begin{cases} 1 & \text{if } \max_i \left\{ |\gamma_i| \right\} > C \\ 0 & \text{otherwise} \end{cases} \qquad (29)$$

An objective function which combines the optimization criteria can then be expressed as:

$$Q = RS + T(1 - S) \qquad (30)$$

The optimization problem is then solved subject to problem constraints. One critical problem constraint is that the shear force applied to the terrain cannot exceed the maximum amount of shear that the terrain can bear, as determined from the relation $T^m = A\left(c + \sigma_m \tan\phi\right)$ where A is the projected wheel area [2]. The parameters c and ϕ are determined from the estimation methods presented above.

Results for a six-wheeled rover traversing rough terrain are shown in Figure 12. In this example the algorithm remains in traction maximization mode, and it can be seen that the rover wheel thrust is increased compared to individual-wheel velocity control by an average of 82%. Here, thrust was measured by an on-board force sensor attached to a weighted sled.

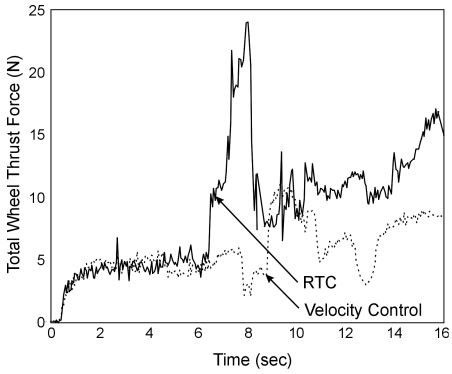

Figure 12: Rough-Terrain control thrust improvement

4.2 Articulated Suspension Control

To meet challenging future mission requirements, robots with actively articulated suspensions have been developed that can improve rough-terrain mobility by modifying their suspension configuration and thus repositioning their center of mass. One example of an articulated suspension robot is the Jet Propulsion Laboratory's Sample Return Rover (SRR), see Figure 13.

An algorithm for actively controlling the suspension to maximize rough-terrain tipover stability has been developed [11]. Kinematic equations relating suspension joint variables to a rover stability measure are written in closed form. An important part of these equations are the wheel-terrain contact angles, described above. A performance index is defined based on the stability measure, and this function is optimized rapidly using a computationally practical conjugate-gradient optimization algorithm.

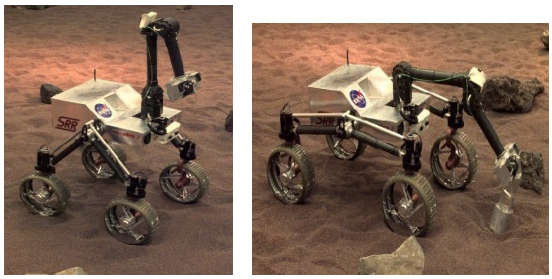

Figure 13: JPL Sample Return Rover

The algorithm has been experimentally validated on the SRR in an outdoor, rough-terrain environment near the Jet Propulsion Laboratory in Pasadena, California. The SRR was commanded to traverse a challenging path that threatened vehicle stability. For each trial the path was traversed first with the rover configuration joints fixed, and then with the articulated suspension control algorithm activated. Rover stability was measured along the path. These results are shown in Figure 14.

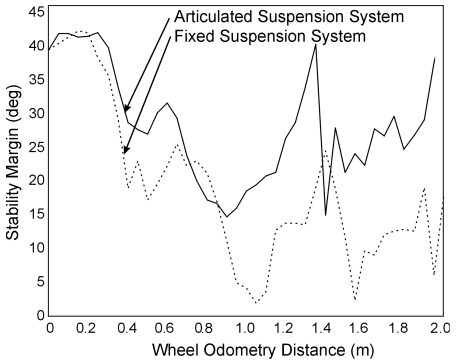

Figure 14: Rough-terrain rover stability improvement

The average stability of the articulated suspension system was 48.1% greater than the fixed suspension system. The stability margin of the fixed suspension system reached dangerous minimum values of 2.1° and 2.5°. The minimum stability margin of the articulated suspension system was 15.0°. Clearly, articulated suspension control results in greatly improved stability in rough terrain.

5. Conclusion

This paper has presented an overview of physics-based rover and terrain modeling techniques. Kinematic and force models of a rover were presented, and it was shown that their solution in rough terrain is nontrivial. Methods for on-line estimation of critical terrain parameters and wheel-terrain contact geometry were

also presented, and shown to yield good results on a rover testbed. These modeling and estimation techniques have been used as a basis for advanced control and planning algorithms to improve a rover's rough-terrain mobility.

Acknowledgements

This work is supported by the NASA Jet Propulsion Laboratory under contract number 960456. The authors would like to acknowledge the support of Dr. Paul Schenker, Dr. Eric Baumgartner and Dr. Terry Huntsberger at JPL.

References

[1] Bickler, D., "A New Family of JPL Planetary Surface Vehicles," *Missions, Technologies, and Design of Planetary Mobile Vehicles,* pp. 301-306, 1992

[2] Bekker, G., *Introduction to Terrain-Vehicle Systems,* University of Michigan Press, 1969

[3] Chottiner, J., *Simulation of a Six-Wheeled Martian Rover Called the Rocker-Bogie,* M.S. Thesis, The Ohio State University, Columbus, OH, 1992

[4] Eckhardt, H., *Kinematic Design of Machines and Mechanisms*, McGraw-Hill, New York, NY, 1989

[5] Hacot, H., *Analysis and Traction Control of a Rocker-Bogie Planetary Rover*, M.S. Thesis, Massachusetts Institute of Technology, Cambridge, MA, 1998

[6] Hayati, S., Volpe, R., Backes, P., Balaram, J., and Welch, W., "Microrover Research for Exploration of Mars," *AIAA Forum on Advanced Developments in Space Robotics*, 1998

[7] Hung, M., Orin., D., and Waldron, K., "Force Distribution Equations for General Tree-Structured Robotic Mechanisms with a Mobile Base," *Proceedings of IEEE International Conference on Robotics and Automation,* pp. 2711-2716, 1999

[8] Iagnemma, K., Genot, F., and Dubowsky, S., "Rapid Physics-Based Rough-Terrain Rover Planning with Sensor and Control Uncertainty," *Proceedings of the 1999 IEEE International Conference on Robotics and Automation*, Detroit, 1999

[9] Iagnemma, K., and Dubowsky, S., "Vehicle Wheel-Ground Contact Angle Estimation: with Application to Mobile Robot Traction Control," *7th International Symposium on Advances in Robot Kinematics, ARK '00*, 2000

[10] Iagnemma, K., and Dubowsky, S., "Mobile Robot Rough-Terrain Control (RTC) for Planetary Exploration," *Proceedings of the 26th ASME Biennial Mechanisms and Robotics Conference, DETC 2000,* 2000

[11] Iagnemma, K., Rzepniewski, A., Dubowsky, S., Huntsberger, T., Pirjanian, P., Schenker, P., "Mobile Robot Kinematic Reconfigurability for Rough-Terrain," *Proceedings of the SPIE Symposium on Sensor Fusion and Decentralized Control in Robotic Systems III,* 2000

[12] Iagnemma, K., *Rough-Terrain Mobile Robot Planning and Control with Application to Planetary Exploration,* Ph.D. Thesis, Massachusetts Institute of Technology, Cambridge, MA, 2001

[13] Plackett, C., "A Review of Force Prediction Methods for Off-Road Wheels," *Journal of Agricultural Engineering Research,* Volume 31, pp. 1-29, 1985

[14] Schenker, P., Sword, L., Ganino, G., Bickler, D., Hickey, G., Brown, D., Baumgartner, E., Matthies, L., Wilcox, B., Balch, T., Aghazarian, H., and Garrett, M., "Lightweight Rovers for Mars Science Exploration and Sample Return," *Proceedings of SPIE XVI Intelligent Robots and Computer Vision Conference*, Volume 3208, pp. 24-36, 1997

[15] Sreenivasan, S., *Actively Coordinated Wheeled Vehicle Systems,* Ph.D. Thesis, The Ohio State University, Columbus, OH, 1994

[16] Sreenivasan, S., and Waldron, K., "Displacement Analysis of an Actively Articulated Wheeled Vehicle Configuration with Extensions to Motion Planning on Uneven Terrain," *Transactions of the ASME Journal of Mechanical Design*, Volume 118, pp. 312-317, 1996

[17] Vincent, E. "Pressure Distribution on and Flow of Sand Past a Rigid Wheel, *Proceedings of the First International Conference on Terrain-Vehicle Systems*, pp. 859-877, 1961

[18] Welch, G., and Bishop, G., "An Introduction to the Kalman Filter," Technical Report TR 95-041, Department of Computer Science, University of North Carolina at Chapel Hill, 1999